



Design of second-order 121.6-nm narrowband minus filters using asymmetrically apodized thickness modulation

Xiaodong Wang¹ · Bo Chen¹ · Tonglin Huo² · Hongjun Zhou²

Received: 20 November 2017 / Accepted: 13 June 2018 / Published online: 19 June 2018
© Springer-Verlag GmbH Germany, part of Springer Nature 2018

Abstract

An asymmetrically apodized thickness modulation design method is proposed to design second-order narrowband minus filters at 121.6 nm. The sine-wave, linear, quintic functions are used as amplitude envelope to apodize the thickness modulation design. LaF₃/MgF₂ minus filters at 121.6 nm with a bandwidth of 5 nm are obtained. This designed filter will be fabricated for utilizing in Lyman-alpha coronagraph and imager installed in Lyman-alpha Solar Telescope, which will be launched by China in 2021.

1 Introduction

The Lyman- α line at 121.6 nm is emitted by hydrogen, which is the strongest line in solar spectrum. This line is cold, and intense, which is formed in solar chromosphere, and it is very sensible to temperature of the chromosphere and magnetic field of chromosphere. The imaging detection of 121.6 nm will provide abundant information about coronal magnetic field, solar eruption, and chromosphere, which plays a very important role in solar and coronal physics [1, 2]. To suppress other solar radiation lines, 121.6 nm minus filters with a narrow bandwidth are needed.

Minus filters, also named as notch filters, are reflective filters. Al/MgF₂/Os multilayer was prepared by Acton Research Company, which was used in the Multi-Spectral Solar Telescope Array. This multilayer has a peak reflectance of 51% at 121.6 nm, and a bandwidth of 15 nm [3]. LaF₃/MgF₂ multilayer was fabricated by Park group, which was utilized in a Ritchey–Chretien Lyman- α telescope. They achieved a net throughput of 27% at 121.6 nm with a bandwidth of 6 nm by utilizing two combination mirrors. They gave a first-order design with $L/H=3$ (where L denotes

optical thickness of low-index material, and H denotes optical thickness of high-index material) [4].

Generally, two methods are employed to narrow down the bandwidth of reflective filter. One is to change the ratio of L/H or H/L , as Park group did. Restricted by available physical thickness, the smallest of the bandwidth for first-order periodic LaF₃/MgF₂ multilayer is calculated to be 10 nm. The other one is to use high-order multilayer [5], and it has a twice or more thicker thickness than first-order multilayer, which gives a more adjusting space for changing the ratio of L/H or H/L . The latter always can get a narrower bandwidth than the former method, but another reflective band will emerge for the latter method.

To suppress other solar radiation lines, the ripples of sidelobe of 121.6 nm stopband should be as low as possible. Some effective methods are developed to reduce the ripples in the passband [6–9]. Perilloux systematically proposed an apodized thickness modulation design (TMD) method to eliminate the sidelobe ripples. They applied amplitude modulation and Gaussian envelope function to TMD. This method was derived from the rugate design. Rugate filter has a continuous variation of the sinusoidal refractive-index profile [10–12]. Southwell imposed amplitude modulation (linear, Gaussian, quintic apodization) on refractive-index profile to further suppress sidelobe reflectance [11, 12]. While apodized thickness modulation design aims to adjust thickness of layers for achieving targeted spectral response. Zhang discussed amplitude modulated (AM)-TMD in reducing the sidelobe ripples of mirrors. He used three kinds of amplitude envelope functions: sine-wave, linear, and quintic functions [13, 14].

✉ Xiaodong Wang
wangxiaodong@ciomp.ac.cn

¹ State Key Laboratory of Applied Optics, Changchun Institute of Optics, Fine Mechanics and Physics, Chinese Academy of Sciences, Changchun 130033, China

² National Synchrotron Radiation Laboratory, University of Science and Technology of China, Hefei 230026, China

In 2021, China will launch Lyman-alpha Solar Telescope, on which Lyman-alpha coronagraph and imager are installed. 121.6-nm narrowband reflective filters are urgent demanded in Lyman-alpha coronagraph and imager.

In this paper, AM-TMD is utilized to design narrow-band minus filter at 121.6 nm, and sine-wave, linear, and quintic functions, respectively, are used as amplitude envelope functions to suppress the ripples on both sides of the 121.6 nm stopband.

2 Design

LaF₃ (*H*) and MgF₂ (*L*) are used in this design, and optical constants are obtained by characterization of absolute reflectance (10°, 20°), transmittance (0°) curves. Optical performances of films in 115–133 nm are measured by National Synchrotron Radiation Laboratory, 134–380 nm by McPherson VUVaS 2000, 381–760 nm by Lambda 1050 UV/VIS/NIR Spectrophotometer. The substrate is fused silica with a thickness of 1.5 mm, the reflectance of backside of the substrate is not taken into account because it is single-side polished. Film thickness is about 200 nm. When fitting T and R, inhomogeneous layer model is utilized, and the used dispersion law for refractive index is normal (Cauchy) dispersion model, the utilized absorption law for extinction coefficient is arbitrary dispersion model in OptiLayer software [15]. The details will be discussed in our next publication. Figure 1 shows our used optical constants of LaF₃ and MgF₂. The extinction coefficient of MgF₂ is higher than that of LaF₃, which is similar to Bischoff's result [16]. The reason for high absorption of MgF₂ may be extrinsic effects, that is, possibly incorporated or adsorbed contaminations, such as hydrocarbons, which would result in additional absorption and maybe also scatter losses in the given spectral range.

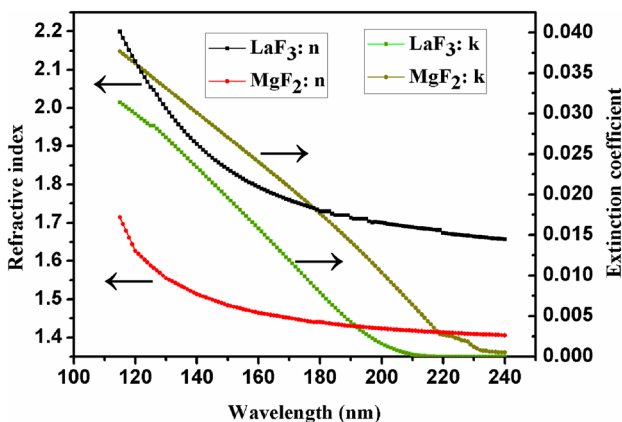


Fig. 1 Optical constants of LaF₃ and MgF₂

2.1 TMD

Generally, in one period of a multilayer, $H+L=0.5\lambda$. When $H/L=1$, its second-order harmonic stopband will disappear if dispersion is absent; a weak second-order rejection band will emerge if dispersion is present. Thus, we do not select quarter-wave multilayer. Additionally, a high ratio of H/L or L/H will result in a narrow bandwidth. Our multilayer is designed by TMD, and its discrete layer thickness is calculated by (1) [9]:

$$T(L) = T_{AVG}[1 + k \cos(2\pi f_m L)], \tag{1}$$

where $T(L)$ is the optical thickness of the L -layer, T_{AVG} is the quarter-wave optical thickness, k is the modulation amplitude, which is the ratio of L/H , and f_m is the modulation frequency. $f_m = 0.5$ is selected in our discussion because this degenerated TMD case has the lowest number of possible rejection zones between first- and second-order stopband. $k=L/H=0.6/1.4$ is selected. The multilayer structure is sub/(0.3L1.4H0.3L)¹¹/air. The total number of layers is 23.

2.1.1 Determination of central wavelength

Due to dispersion of material in far ultraviolet, there is no simple multiple relationships between first- and high-order reflection zones. The central wavelength is determined by (2) [9]:

$$\sigma_{M,N} \approx \frac{\sigma[2Nf_m + (2M - 1)]}{1 + \frac{1}{2} \left(\frac{\Delta n_L}{nL_0} + \frac{\Delta n_H}{Nn_0} \right)}, \tag{2}$$

where $\sigma_{M,N}$ is the higher order stopband (wavenumber, nm^{-1}), σ_0 is the first-order rejection zone, M and N are the integer numbers, Δn_i is the refractive index variance of high- and low-index materials due to dispersion of materials, and n_{i0} is the refractive index of high- and low-index materials at fundamental rejection zone.

In this paper, $f_m = 0.5, M = 1, N = 1, \sigma_{M,N} = \sigma_{1,1} = 1/121.6 \text{ nm}$. Now we should determine σ_0 . The reasons for the values we employed here can be found in [9]. Due to space reasons, here we do not provide the detailed explanations.

Owing to dispersion of materials in this wavelength range, $\Delta n_i/n_{i0}$ is introduced into this formula. Curves of optical constants for LaF₃ and MgF₂ are fitting by first-order exponential decay (3):

$$y = A_1 \exp(-x/t) + y_0, \tag{3}$$

where A_1, t , and y_0 are the constants, and x is the wavelength. The fittings are shown in Fig. 2, and the results are described by (4).

$$\begin{aligned} y_H &= 16.965 \exp(-x/33.410) + 1.653 \\ y_L &= 21.011 \exp(-x/26.460) + 1.411. \end{aligned} \tag{4}$$

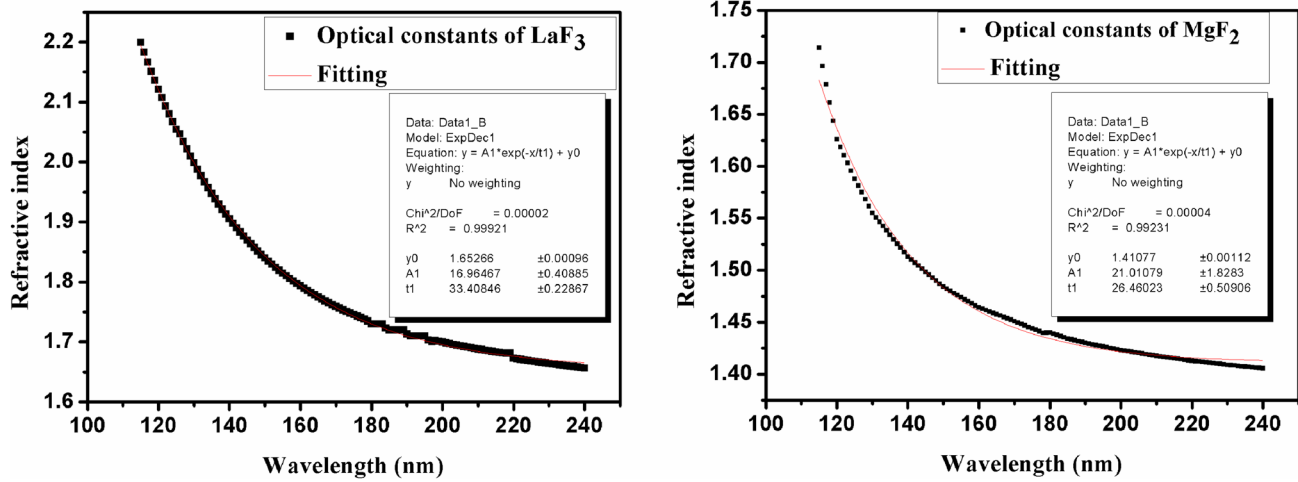


Fig. 2 Fittings of optical constants for LaF₃ (left) and MgF₂ (right) by first-order exponential decay

Taken LaF₃ as an example ($n_{121.6\text{nm}} = 2.094$), $\Delta n_H/n_{H_0}$ can be calculated as below:

$$\begin{aligned} \frac{\Delta n_H}{n_{H_0}} &= \frac{2.094 - 16.965 \exp(-x/33.410) - 1.653}{16.965 \exp(-x/33.410) + 1.653} \\ &= \frac{2.094}{16.965 \exp(-x/33.410) + 1.653} \\ -1 &\approx \frac{2.094}{1.653} - 1 = 0.267. \end{aligned}$$

The value of $\Delta n_L/n_{L_0}$ is calculated using the same method to be 0.1416. Finally, σ_0 is determined to be 1/202, which means the central wavelength is 202 nm. The calculated central wavelength using (2) is very close to the exact value of 203 nm, which is obtained by OptiLayer software [15] using trial and error method.

2.1.2 TMD Result

Figure 3 shows theoretical reflectance curve of periodic multilayer (sub/(0.3L1.4H0.3L)¹¹/air), here $k = 0.6/1.4$, $f_m = 0.5$. We can see that there are ripples on the right sides of 121.6 nm rejection zone, which needs to be further reduced, and the bandwidth is 7 nm.

2.2 AM-TMD

AM-TMD is used to suppress the ripples on the right sides of 121.6 nm stopband, and Eq. 5 gives the calculation of discrete layer thickness:

$$T(L) = T_{\text{AVG}}[1 + kA(L) \cos(2\pi f_m L)]. \tag{5}$$

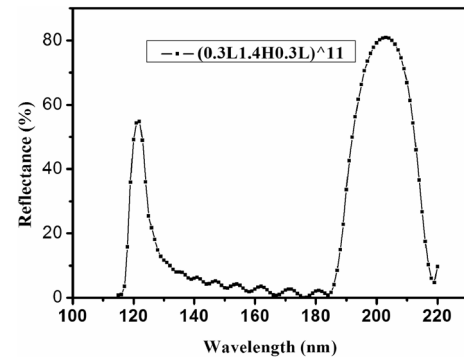


Fig. 3 Theoretical reflectance curve of periodic multilayer (sub/(0.3L1.4H0.3L)¹¹/air)

where $A(L)$ is the amplitude envelope function, and it can be sine-wave, linear, quintic functions. It is noted that our amplitude envelope functions are same to Zhang [13], and Zhang did not clearly give the description of $f_m = 0.5$.

2.2.1 Sine-wave AM-TMD

Sine-wave amplitude envelope function is described by (6), where L_{TOT} is the total number of AM layers, not the whole multilayer.

$$\begin{aligned} A(L) &= \sin(2\pi f_1 L) \\ f_1 &= \frac{1}{2L_{\text{TOT}}}. \end{aligned} \tag{6}$$

Figure 4 demonstrates theoretical reflectance curves of left side, right side, and both side AM-TMD of multilayer (seven layers apodization). Left side AM-TMD gives no changes, and right side AM-TMD provides best sidelobe

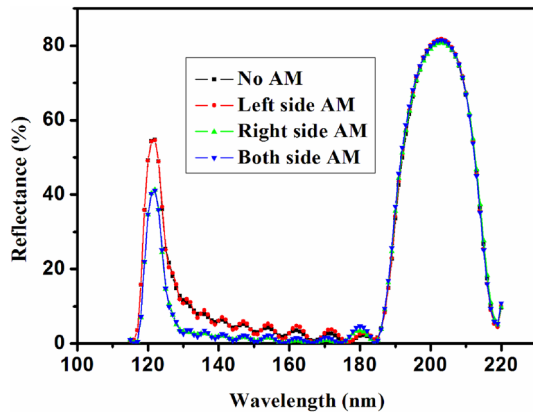


Fig. 4 Theoretical reflectance curves of left side, right side, and both side AM-TMD of multilayer (seven layers apodization)

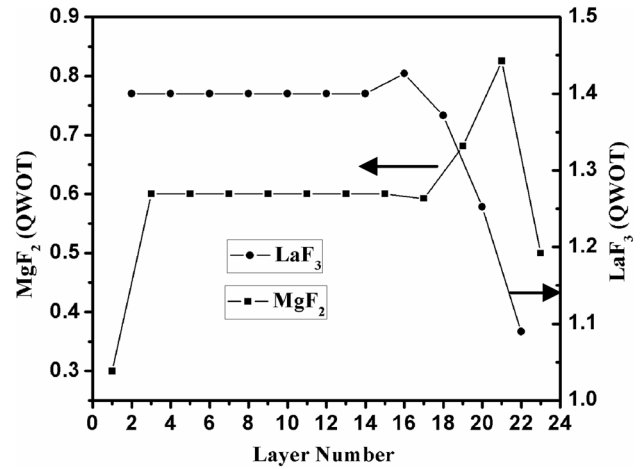


Fig. 6 Thickness distribution of discrete layers of seven layers apodization of multilayer

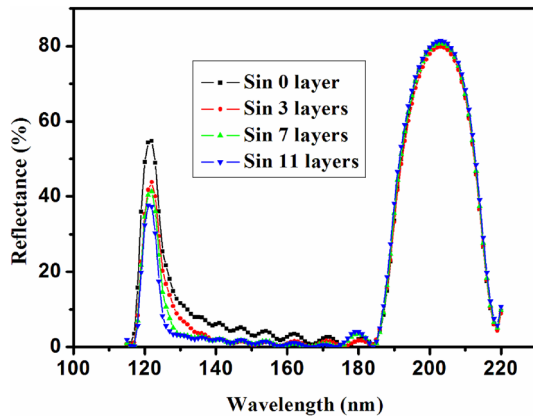


Fig. 5 Theoretical reflectance curves of right side sine-wave AM-TMD of multilayer (zero, three, seven, and eleven layers apodization)

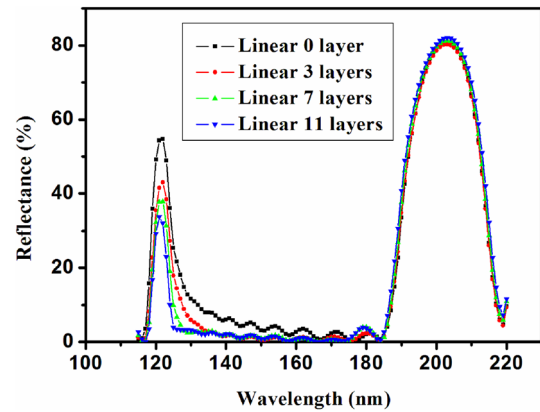


Fig. 7 Theoretical reflectance curves of right side linear AM-TMD of multilayer (zero, three, seven, and eleven layers apodization)

suppression. Linear and quintic envelope functions also have similar situations. Thus, in this paper, we choose right side AM-TMD.

Figure 5 reveals theoretical reflectance curves of right side AM-TMD of multilayer. Here, for brevity, only zero, three, seven, and eleven layers apodizations are drawn. We can see that with the increasing of number of apodized layers, bandwidth gets narrower. Finally, due to eleven layers AM-TMD, a minus filter with a bandwidth of 5 nm is obtained, and its peak reflectance is 37.6% at 121.6 nm.

Figure 6 shows thickness distribution of discrete layers of seven layers apodization of multilayer. Quarter wave optical thicknesses (QWOT) of LaF₃ and MgF₂ are 1.09–1.426 and 0.3–0.825, respectively. The physical thicknesses are from 10 nm to 42 nm. There are significant thickness changes at right side (near to air) than left side (near to substrate).

2.2.2 Linear AM-TMD

Linear amplitude envelope function is described by (7), and t is determined by (8). Figure 7 demonstrates theoretical reflectance curves of right side linear AM-TMD of multilayer. Here, for clarity, only zero, three, seven, and eleven layers apodizations are drawn. We can see that with the increasing of number of apodized layers, bandwidth gets narrower. Finally, due to eleven layers AM-TMD, a minus filter with a bandwidth of 5 nm is obtained, and its peak reflectance is 33.9% at 121.6 nm.

$$A(L) = 4f_1 t, \tag{7}$$

$$t = \begin{cases} L & \text{for } L \leq L_{TOT}/2 \\ L_{TOT} - L & \text{for } L > L_{TOT}/2 \end{cases} \tag{8}$$

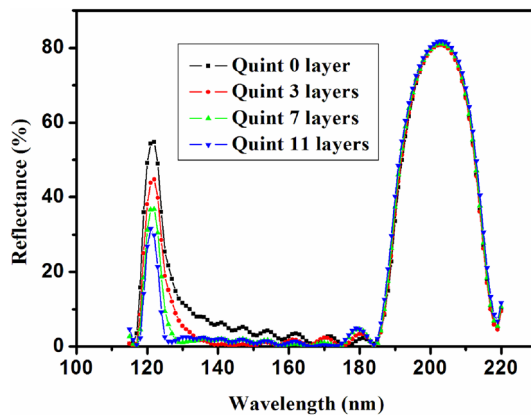


Fig. 8 Theoretical reflectance curves of right side quintic AM-TMD of multilayer (zero, three, seven, and eleven layers apodization)

2.2.3 Quint AM-TMD

Quintic amplitude envelope function is described by (9), and m is determined by (10). Figure 8 shows theoretical reflectance curves of right side quintic AM-TMD of multilayer. Here, for brevity, only zero, three, seven, and eleven layers apodizations are drawn. We can see that with the increasing of number of apodized layers, bandwidth gets narrower. Finally, due to eleven layers AM-TMD, a minus filter with a bandwidth of 5 nm is obtained, and its peak reflectance is 29.9% at 121.6 nm.

$$A(L) = 10m^3 - 15m^4 + 6m^5, \quad (9)$$

$$m = 4f_1 t. \quad (10)$$

2.2.4 Comparison

For comparison, theoretical reflectance curves of three kinds (sine-wave, linear, and quintic functions) of AM-TMD (seven layers apodization) were drawn in Fig. 9. Multilayer with a best spectral performance is achieved using quintic envelope function AM-TMD, and it has a bandwidth of 5 nm, a peak reflectance of 36.7 nm in 1.6 nm, and a good sidelobe suppression. Similar results were also achieved by Rugate design in Southwell's jobs [11, 12], but their index modification needs precise control, which is very difficult in deposition, and thickness modulation is much more easier to be carried out than index modification in practice.

3 Conclusion

Right side AM-TMD, as an asymmetrically apodization, exhibits a good, even slightly better spectral response than both side AM-TMD in far ultraviolet waveband, which is not

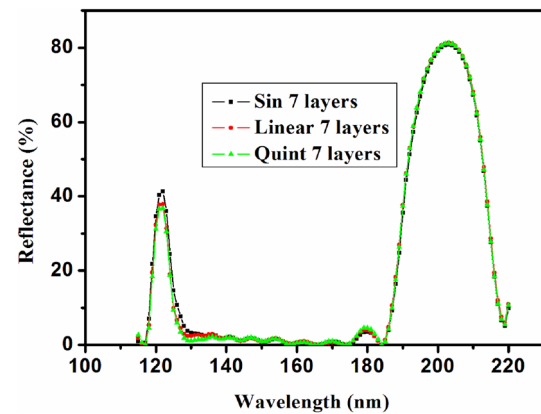


Fig. 9 Theoretical reflectance curves of three kinds (sine-wave, linear, and quintic functions) of AM-TMD (seven layers apodization)

observed in designing filters in visible waveband. A modified Perilloux's method provides a precise determination of central wavelength.

A second-order minus filter at 121.6 nm was designed by AM-TMD method, and it has a bandwidth of 5 nm, a reflectance of more than 30%. The bandwidth of our one mirror is similar to Park's theoretical results of two combination mirrors, but our mirror has better sidelobe suppression. However, it has a lower reflectance. In addition, a high reflectance at 203 nm is a big shortcoming for our minus filters, which needs a transmission filter (such as Acton 122N filter) or a first order of 121.6-nm minus filter to eliminate. Although computer software of optical thin film design is very strong in designing filters today, a good preliminary design is still required, which will contribute most to the outcome of a best design. Our proposed method can provide a good preliminary design for further optimization of computer software.

Acknowledgements This work is supported by the Joint Research Fund in Astronomy (U1531106) under cooperative agreement between the National Natural Science Foundation of China (NSFC) and Chinese Academy of Science (CAS), partially supported by NSFC (Grant No.11427803), and partially supported by the Strategic Priority Research Program of Chinese Academy of Science (CAS), Grant No. XDA15320103.

References

1. B. Li, H. Li, S. Zhou, B. Jiang, Proc. of SPIE **9042**, 90420Y, (2013)
2. S. Vives, P. Lamy, J. Vial, Proc. of SPIE **5171**, pp. 298–306, (2004)
3. R.B. Hoover, T.W. Barbee, J.P.C. Baker, J.F. Lindblom, M.J. Allen, C.D. Forrest, C. Kankelborg, R.H. O'Neal, E. Pairis, A.B.C. Walker, Opt. Eng. **29**(10), 281–290 (1990)
4. J.H. Park, M. Zukic, M. Wilson, C.E. Keffer, D.G. Torr, R.B. Hoover, Opt. Eng. **35**(5), 1479–1482 (1996)

5. H.A. Macleod, *Thin-Film Optical Filters*, 4th edn. (CRC Press, Boca Raton, 2010)
6. A. Thelen, *J. Opt. Soc. Am.* **61**, 365–369 (1971)
7. B.E. Perilloux, *Appl. Opt.* **37**, 3527–3532 (1998)
8. B.E. Perilloux, *Appl. Opt.* **38**, 2911–2915 (1999)
9. B.E. Perilloux, *Thin-Film Design: Modulated Thickness and Other Stopband Design Methods*, (SPIE Press, Bellingham, 2002)
10. B.G. Bovard, *Appl. Opt.* **29**, 24–30 (1990)
11. W.H. Southwell, R.L. Hall, *Appl. Opt.* **28**, 2949–2951 (1989)
12. W.H. Southwell, *Appl. Opt.* **28**, 5091–5094 (1989)
13. J.L. Zhang, Y.J. Xie, X.B. Cheng, H.F. Jiao, Z.S. Wang, *Appl. Opt.* **52**(23), 5788–5793 (2013)
14. J.L. Zhang, A.V. Tikhonravov, M.K. Trubetskov, Y.L. Liu, X.B. Cheng, Z.S. Wang, *Opt. Express* **21**(18), 21523–21529 (2013)
15. A.V. Tikhonravov, M.K. Trubetskov, OptiLayer thin film software. <http://www.optilayer.com>. Accessed 15 June 2017
16. M. Bischoff, O. Stenzel, K. Friedrich, S. Wilbrandt, D. Gäbler, S. Mewes, N. Kaiser, Plasma-assisted deposition of metal fluoride coatings and modeling the extinction coefficient of as-deposited single layers. *Appl. Opt.* **C232**, 50 (2011)